

Marine ecological damage assessment model for offshore oil extraction

Qingjing Yang and Hongyuan Liu

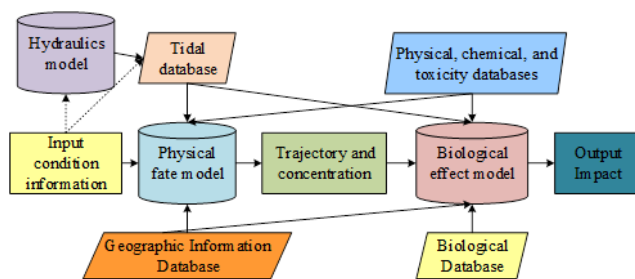
School of Economics and Management, Southwest Petroleum University, Chengdu, 610500, China

Received: 18/04/2024, Accepted: 07/07/2024, Available online: 24/07/2024

*to whom all correspondence should be addressed: e-mail: liuhongyuan0813@sina.com

<https://doi.org/10.30955/gnj.006076>

Graphical abstract



Abstract

With the progress of society and the development of the economy, people's awareness of environmental protection is also becoming stronger. Therefore, the damage caused by marine oil spills caused by offshore oil extraction to marine ecology is also receiving more and more attention from people. Marine ecological damage assessment involves various disciplines such as environmental chemistry, biology, toxicology, and hydrodynamics, and requires a large amount of data support, making it a challenge in the field of marine claims. To quantitatively evaluate marine oil spill accidents, the Spill Impact Model Application Package model is used as the system framework to build a marine ecological damage assessment model. The MIKE21 model is used for physical fate simulation, while the biological effects model is used for resource damage assessment of the ecological environment and aquatic organisms. The model is validated using the oil spill accident in Dongshan Bay as an example. The validation results show that the total loss of aquatic organisms under conditions 1 and 2 is 67.30 tons and 56.03 tons, respectively. Under condition 1, the ecological environment of coral and mangroves is affected by an area of 8.805km² and 5.859km², respectively, resulting in a loss of 19.5168 million yuan in ecological resources. Under condition 2, the ecological environment of coral and mangroves is affected by an area of 7.646 km² and 13.515 km², respectively, resulting in a loss of 26.322 million yuan in ecological resources. In summary, it can be seen that the research on marine ecological damage assessment models for offshore oil extraction provides

certain reference value for the field of marine ecological damage assessment in China.

Keywords: Marine oil spill; assessment model; ecological damage; oil extraction; simap model

1. Introduction

With the continuous growth and expansion of offshore oil trade and oil extraction activities, marine oil spills often occur, causing serious damage to marine ecology. However, due to the lack of a reasonable and objective marine ecological damage assessment (MEDA) model, China often does not receive the necessary compensation (Chassé and Blatrix 2020). The ecological damage caused by oil spills is reflected in both the ecological environment and marine organisms. After oil spills occur, oil will exist in various forms such as emulsified oil, dissolved oil, floating oil, and attached oil in the ocean, posing a serious threat to marine organisms and the marine ecological environment, and even leading to the imbalance of the entire marine ecosystem. The assessment of marine ecological damage in foreign countries started early and has established relatively complete methods for MEDA. Among them, the most common methods are computer modeling method and empirical formula method (Veklych *et al.* 2020; Nazuk *et al.* 2021). China began to gradually research and explore methods for assessing marine ecological damage in the 1990s. However, when conducting ecological damage assessments, China often roughly estimates the loss of biological resources based on the concentration of oil spills on the surface of seawater, and does not evaluate the loss from different perspectives such as marine organisms, exposure temperatures, and exposure times. Therefore, the existing MEDA methods in China are not comprehensive enough to a certain extent, resulting in insufficient compensation efforts (Ardiada *et al.* 2022). Meanwhile, in recent years, China's MEDA models have focused on whole oil as the research object. However, the oil extracted from the sea belongs to different hydrocarbon mixtures, and the physicochemical properties produced by different hydrocarbon substances in complex marine environments also vary greatly. Therefore, marine organisms and marine ecology are not in a whole oil environment. Studying the assessment of marine

ecological damage based on whole oil often leads to deviations in the assessment results (Lima *et al.* 2022). In this context, a MEDA model for offshore oil extraction is studied to establish a more comprehensive MEDA method. The research content mainly includes four parts. The second part is a review of the research status of MEDA methods and the Spill Impact Model Application Package (SIMAP) model both domestically and internationally. The third part conducted the construction of a SIMAP-based MEDA model for offshore oil extraction. The first section studied the construction of a SIMAP-based MEDA model, and the second section conducted the physical fate simulation design of a SIMAP-based MEDA model. The fourth part provides an example analysis of the marine ecological loss assessment model for offshore oil extraction.

2. Related works

MEDA can quantitatively assess the ecological damage caused by offshore oil extraction, which has attracted the attention of many researchers both domestically and internationally. Researchers such as R.J. Wenning proposed to initiate a preliminary damage assessment program during wartime that can predict and record the severity of damage to scientifically and systematically evaluate environments damaged by war. This program incorporated the EU Environmental Responsibility Directive on the basis of the US Natural Resource Damage Assessment System, and the results showed that this program was applicable for assessing ecological damage during armed conflicts (Wenning, and Tomasi 2023). In order to improve the reliability and detail of life cycle impact assessment methods, scholars such as Verones *et al.* (2020) proposed an improved life cycle impact assessment method. This method quantified human health damage, mineral resource damage, and ecosystem quality damage, and the outcomes denoted that this method was feasible in the field of life cycle assessment. To improve the reliability and accuracy of structural health monitoring systems, Kralovec and Schagerl (2022) research team proposed to combine conductivity monitoring systems with other sensors to construct a structural health monitoring system based on multiple powerful sensors. The system was used to experimentally validate the structure of composite materials, and the experimental findings indicated that the system effectively improved monitoring performance. Researchers such as E.K. Rowen proposed a comprehensive pest management method to address pest risks and avoid crop damage from pests. To avoid pesticide damage to crops, this method did not use pesticides, but instead responds to pest risks by planting cover crops. The research results expressed that planting early season cover crops was more effective than any other pest intervention strategy (Rowen *et al.* 2022).

The physical fate simulation in the SIMAP model plays an important role in the field of MEDA. E. Dukes' research team proposed improvements to the nitrogen footprint assessment method and tools to study the relationship between nitrogen cycling, resource consumption, and environmental impact. This method combined nitrogen

and carbon footprints using the SIMAP, and compared the footprint results evaluated by this method with those of seven other institutions. The results showed that this method effectively improved the accuracy of footprint assessment results (Dukes *et al.* 2021). Bigdeli *et al.* (2022) proposed a water quality particle tracking module to simulate and track microplastic particles to study the impact of microplastic pollution on marine organisms and water resources. The model structure included four famous Lagrangian particle tracking modules, including Canadian plastic tracking, fish scale plankton tracking, water quality particle tracking, and marine plastic debris tracking. The results denoted that this method was feasible in the field of marine microplastic pollution research (Bigdeli *et al.* 2022). K.L. Ng *et al.* (2021) proposed a desktop quantum simulator based on the engineering Bose Einstein condensate form to address the exponential complexity in studying quantum theory problems. The simulator used the approximately truncated Wigner phase space method to analyze the numerical values of the simulator under real conditions. The results showed that the simulator could analyze the non local observable values of topological phase entropy (K.L. Ng *et al.* 2021). Li *et al.* (2021) proposed a physiological pharmacokinetic model with phagocytosis to study the dynamics of nanoparticles between organs in organisms. The model incorporated cellular mechanisms with retention effects into the model structure to enhance permeability. The results showed that this model could analyze the complex transport mechanism of nanoparticles in the body.

In summary, domestic and foreign scholars have conducted a large amount of research using ecological damage assessment methods and SIMAP models, but there is relatively little research on quantitative assessment of marine ecological damage. Therefore, the study focuses on the MEDA model for oil extraction in Shanghai, to provide a certain reference for the assessment of marine ecological losses in China.

3. SIMAP-based MEDA model for offshore oil extraction

The SIMAP model is the foundation and prerequisite for subsequent research in this article. This chapter focuses on the design and construction of the biological effects model and physical fate model in the SIMAP model structure, and uses the MIKE21 model for physical fate simulation. The ecological environment equivalence analysis method is also used to evaluate the ecological environment resource loss in the biological effects model. At the same time, the effectiveness of the model is verified and explained through examples.

3.1. Construction of a SIMAP-based MEDA model

The SIMAP is a marine oil spill impact model that covers both biological effects and physical fate models. This model can use biological effects models to evaluate the biological damage caused by oil spills, and can use physical fate models to simulate the concentration of oil components and oil spill trajectories in water bodies (Yool *et al.* 2021). The system structure of the SIMAP model is shown in Figure 1.

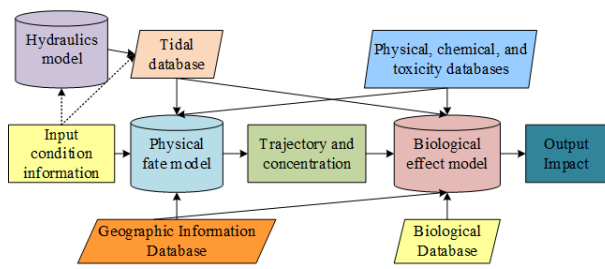


Figure 1. System structure diagram of SIMAP model

As shown in Figure 1, when using the SIMAP model for MEDA, it is necessary to first input wind conditions and scene information during oil spills, and use data

information such as wind speed and temperature at that time to simulate and analyze tidal current operation and oil spill trajectory in hydraulic and physical fate models. At the same time, biological effects are analyzed based on the physical, chemical, and toxic characteristics of oil. The physical fate model can simulate the random dispersion, evaporation, entrainment, emulsification, and dissolution of spilled oil on the sea surface, as oil is a complex mixture of hydrocarbons composed of different physical, chemical, and toxic characteristics. Therefore, different hydrocarbons in oil will have different impacts on marine life. The fate of oil spills in the ocean is shown in Table 1.

Table 1. The fate of oil spills in the ocean

Oil spill destination	Duration/d	Proportion/%
Volatilize	1-10	25
Dissolve	1-10	5
Biodegradation	50-500	30
Dispersion and settlement	100-1000	15
Photochemical reaction	10-100	5
Residual	>100	20

To more accurately evaluate ecological damage, the SIMAP model uses the pseudo component method to group oils according to their physical and chemical properties. According to the hydrophobicity, solubility, and evaporation of the oils, the spilled oil is divided into eight pseudo components: residual aliphatic hydrocarbons, residual aromatic hydrocarbons, semi volatile aliphatic hydrocarbons, volatile aliphatic hydrocarbons, low volatile aliphatic hydrocarbons, and monocyclic, bicyclic, and tricyclic aromatic hydrocarbons. Among these eight pseudo components, the toxicity and water solubility of aromatic hydrocarbon spills are much greater than those of fatty hydrocarbon spills. Therefore, when calculating the concentration of water bodies using physical fate models, only the pseudo component concentration of soluble aromatic hydrocarbon spills is calculated. The process simulation diagram of the physical fate model is shown in Figure 2.

coastline based on the type of coastline, and simulate the diffusion, evaporation, emulsification, dissolution, adsorption, and entrainment of oil based on the structure of the oil spill. Volatilization and degradation have various physical consequences (Rosti *et al.* 2021). The results simulated by the physical fate model generally include data such as the thickness of the oil film on the sea surface, the concentration of total hydrocarbons attached to suspended particles, the concentration of dissolved aromatic hydrocarbons in seawater, the concentration of soluble aromatic hydrocarbons, the concentration of total hydrocarbons present in surface sediments, and the location and length of the coastline contaminated by oil spills. These data will be applied to the analysis of the biological effects model, to further evaluate the damage to marine ecology. The biological effect model is mainly used to evaluate the production losses caused by the death of marine organisms and food chain faults after oil spill accidents. The structural diagram of the biological effect model is shown in Figure 3.

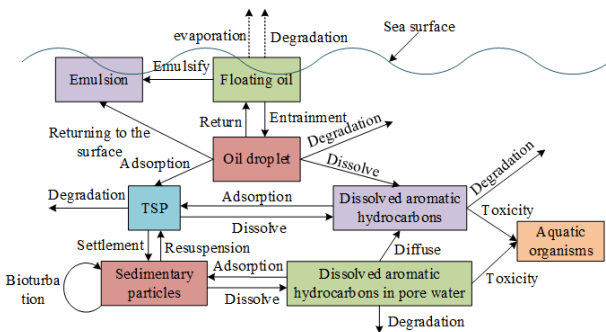


Figure 2. Process simulation diagram of physical fate model

As shown in Figure 2, the physical fate model can simulate the motion trajectories of oil spill components, surface oil slicks, and suspended oil droplets in space based on the horizontal flow velocity, random turbulent diffusion velocity, and surface wind induced flow of the ocean. It can analyze and determine whether the oil spill adheres to the

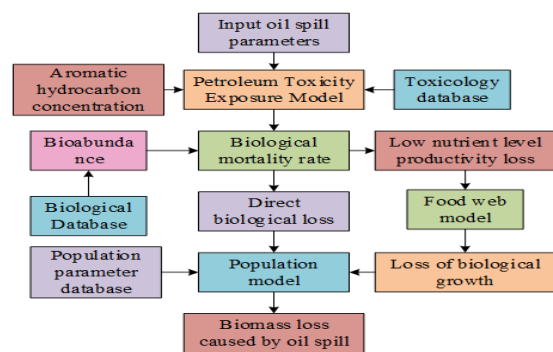


Figure 3. Structure diagram of biological effect model

As shown in Figure 3, in the structure diagram of the biological effect model, the biological abundance in the biological database is input into the model as input data to calculate more accurate biological loss. The biological

effects model encodes the grid based on the ecological environment type, which includes coastline, seaweed beds, seagrass beds, corals, wetlands, and open water areas. Ecological environment grids with the same code can be considered as an ecosystem, and the productivity generated by the ecosystem before the oil spill is set to a constant value. When simulating in biological effects models, Lagrangian particles are used to represent organisms in the ecological environment, and behavior groups are divided based on their habits and life stages. Based on this, the motion speed and state of particles are set (Abel and Spannowsky 2021). The petroleum toxicity exposure model in the biological effect model structure can evaluate the toxicity of dissolved aromatic hydrocarbons to various organisms. The calculation method for the toxicity concentration in organisms is shown in equation (1).

$$C_o(t) = C_w(t)(\alpha/\beta)(1 - e^{-\beta t}) \quad (1)$$

In equation (1), t means time; $C_o(t)$ represents the toxic concentration in the organism; $C_w(t)$ denotes the toxic concentration in the water, and α and β indicate constants for absorption rate and elimination rate, respectively. In an ideal state, the toxic concentration in the organism and water body should reach equilibrium over time, and the expression for the bioconcentration coefficient at equilibrium is shown in equation (2).

$$B = C_o(\infty)/C_w(\infty) = \alpha/\beta \quad (2)$$

In equation (2), B means the bioconcentration coefficient at equilibrium. At this point, $t = \infty$ sets the concentration $C_o(\infty)$ in the organism at $t = \infty$ as the critical residual concentration. The expression for the toxic concentration in the water environment when the mortality rate of the organism reaches 50% is shown in equation (3).

$$LC50_{(\infty)} = C_w(\infty) = C_o(\infty)/B = A/B \quad (3)$$

In equation (3), A denotes the critical residual concentration within the organism, and $LC50_{(\infty)}$ represents the concentration of water that causes a 50% biological mortality rate at time $t = \infty$. The increase in temperature will accelerate the rate of biological and chemical reactions, and at the same time, temperature will also

affect the absorption, metabolism, and elimination of dissolved aromatic hydrocarbons in organisms, thereby affecting the toxicity of aromatic hydrocarbons to aquatic organisms. Research has found that the toxicity of aromatic hydrocarbons to aquatic organisms increases with the increase in temperature (Maihulla *et al.* 2022). The effect of temperature on the elimination rate is shown in equation (4).

$$\beta(T_2) = \beta e^{(\tau_2 - \tau_1)} \quad (4)$$

In equation (4), T expresses temperature; T_1 and T_2 represent different temperatures; τ indicates a constant. When chemical substances with similar chemical effects are superimposed, the toxicity calculation formula of the mixture is shown in equation (5).

$$LC50_{mix} = 1/\sum(P_i/LC50_i) \quad (5)$$

In equation (5), $LC50_{mix}$ denotes the toxic concentration at which the mixture produces a 50% biological mortality rate, and $LC50_i$ expresses the toxic concentration at which the chemical i produces a 50% biological mortality rate. p_i represents the proportion of chemical substance i in the mixture, i.e. $P_i = C_{w,i} / (\sum C_{w,i})$. When evaluating the mortality rate of aquatic organisms, the SIMAP model mainly considers the impact of dissolved aromatic hydrocarbons on organisms, while when evaluating the mortality rate of wildlife, it is necessary to consider the impact of surface oil slick on organisms (Khan *et al.* 2022). Wildlife includes birds, turtles, and mammals. When the thickness of the surface oil slick exceeds the threshold, it can cause the death of wildlife. This mortality rate is calculated by multiplying the probability of wildlife exposure to oil slicks by the threshold of oil slick thickness at the time of exposure, and the probability of wildlife exposure to oil slicks is also related to biological habits. Related studies have shown that the mortality rate of hairy mammals and birds in contact with oil slicks without artificial treatment has reached almost 100%. The mortality rates of different wildlife exposed to oil slicks are shown in Table 2.

Table 2. Mortality rate of different wildlife exposed to floating oil

Categories	Mortality/%
Whales	0.1
Seabirds in the air	5.6
Sea lions, seals, and turtles	1.2
Birds that dive and prey near shore	35.4
Wetland wildlife	35.1
Marine mammals with fur	75.9
Waterbirds and seabirds on the sea surface	99.3

3.2. Physical fate simulation design of MEDA model based on SIMAP

From the previous section, the output results of the physical fate model are influenced by factors such as horizontal ocean velocity, random turbulent diffusion velocity, and surface wind induced currents. Currently, the

most advanced model internationally that can be used to simulate ocean water flow is the MIKE21 model developed by the Danish Institute of Water Environment, which includes a hydrodynamic module, a pre and post processing module, a water quality and environmental evaluation module, and a sediment transport module. It

can be used for simulating the physical fate of marine ecological damage (Zan 2022). The hydrodynamic module in the MIKE21 model can simulate the changes in ocean tidal current field, and the basic ocean tidal current field equation is shown in equation (6).

$$\begin{cases} \frac{\partial q}{\partial t} + \frac{\partial}{\partial x} \left(\frac{pq}{h} \right) + \frac{\partial}{\partial y} \left(\frac{q^2}{h} \right) + gh \left(\frac{\partial \xi}{\partial x} \right) + \frac{gq\sqrt{p^2+q^2}}{c^2 h^2} - \frac{1}{\rho_w} \left[\frac{\partial(h\tau_{xx})}{\partial x} + \frac{\partial(h\tau_{xy})}{\partial y} \right] \\ -\Omega_p - f_w VV_x + \frac{h}{\rho_w} \times \frac{\partial(P_a)}{\partial x} = 0 \\ \frac{\partial q}{\partial t} + \frac{\partial}{\partial x} \left(\frac{pq}{h} \right) + \frac{\partial}{\partial y} \left(\frac{q^2}{h} \right) + gh \left(\frac{\partial \xi}{\partial y} \right) + \frac{gq\sqrt{p^2+q^2}}{c^2 h^2} - \frac{1}{\rho_w} \left[\frac{\partial(h\tau_{yy})}{\partial y} + \frac{\partial(h\tau_{xy})}{\partial x} \right] \\ -\Omega_p - f_w VV_y + \frac{h}{\rho_w} \times \frac{\partial(P_a)}{\partial y} = 0 \end{cases}$$

In equation (6), p and q represent the flux density in the x and y directions; h represents the total water depth; ξ represents the water surface elevation; c denotes the Chezy coefficient; g represents the gravitational acceleration; Ω_p expresses the Coriolis parameter; f_w indicates the wind resistance coefficient; ρ_w denotes the density of water; P_a means atmospheric pressure; V , V_x , and V_y represent the wind speed, the components of wind speed in the x direction, and wind speed in the y direction, respectively. τ_{xx} , τ_{xy} and τ_{yy} respectively represent the effective shear stress in their corresponding directions. The spreading process of simulated oil spills in the MIKE21 physical fate model is shown in equation (7).

$$\left(\frac{dM_{oil}}{dt} \right) = K_a M_{oil}^{1/3} \left(\frac{V_{oil}}{M_{oil}} \right)^{4/3} \quad (7)$$

In equation (7), M_{oil} and V_{oil} represent the area and volume of the oil spill, respectively, and K_a means the coefficient. The oil spill will drift under the action of water flow and wind flow, and the acceleration of the drift is shown in equation (8).

$$U = \delta_w U_w + \delta_a U_a \quad (8)$$

In equation (8), U represents the speed of drift; U_w denotes the wind speed at a distance of 10 meters from the water surface; U_a denotes the velocity of seawater; δ_w and δ_a represent the coefficients of wind drift and seawater advection, respectively. If the diffusion of oil spill in the horizontal direction is isotropic, the distance generated by oil spill drift in the y direction within a time range can be calculated as shown in equation (9).

$$S_y = [R]_{-1}^1 \times \sqrt{6G_y \Delta t_y} \quad (9)$$

In equation (9), S_y , G_y , and Δt_y mean the distance, coefficient and the time period of diffusion in the y direction, respectively. $[R]_{-1}^1$ represents the random number within the $[-1, 1]$ range. The phenomenon of oil spill evaporation is influenced by various factors such as sunlight exposure, oil spill area, seawater temperature, oil spill components, oil film thickness, and wind speed. The evaporation rate of oil spill is shown in equation (10).

$$E_i = \frac{K_i P_i^{SAT}}{RT} \times \frac{m_i X_i [m^3/m^2 s]}{\rho_i} \quad (10)$$

In equation (10), E_i expresses the evaporation rate; i refers to the component of the spilled oil; K_i represents the mass transfer coefficient; R serves as the gas constant; T denotes the temperature, and P_i^{SAT} represents the vapor pressure. m_i means molecular weight; X_i indicates molar fraction; ρ_i represents the density of the spilled oil. Assuming that the solubility of the spilled oil component is much greater than its hydrocarbon concentration, the solubility of the spilled oil is shown in equation (11).

$$\frac{dR}{dt} = \frac{K_s X_{mol} m_i A_{oil}}{\rho_i} \quad (11)$$

In equation (11), R represents the solubility of the spilled oil; A_{oil} means the area of the spilled oil; X_{mol} refers to the molar fraction of the spilled oil; K_s represents the mass transfer coefficient. Spilled oil in seawater not only undergoes horizontal diffusion, but also vertical dispersion phenomena of downward diffusion and upward return. The rate expression of upward dispersed spilled oil components when returning is shown in equation (12).

$$\begin{cases} F = F_\alpha + F_\beta \\ \frac{dV_{oil}}{dt} = F_\alpha (1 - F_\beta) \\ F_\alpha = \frac{0.11(1 + U_w)^2}{3600} \\ F_\beta = \frac{1}{1 + 50\mu_{oil} h_s \zeta_{ow}} \end{cases} \quad (12)$$

In equation (12), F serves as the vertical dispersion of the spilled oil; F_α means the portion of the spilled oil that produces vertical downward dispersion per second; F_β denotes the portion of the spilled oil that does not return upward after dispersion; V_{oil} represents the rate at which the spilled oil returns; μ_{oil} expresses the viscosity of the spilled oil; h_s indicates the thickness of the oil film, and ζ_{ow} represents the tension at the contact surface between the sea water and the spilled oil. After oil spills come into contact with water and interact with each other, emulsification occurs, forming an emulsion in the form of oil in water. The water content in the emulsion is generally greater than 80%, which increases the viscosity of the oil spill and causes it to persist on the sea surface for a long time. The expression for the absorption and release rate of water in the emulsion is shown in equation (13).

$$\begin{cases} R_\alpha = \frac{\varphi_\alpha (1 + U_w)^2}{\mu_{oil}} \times (y_w^{max} - y_w) \\ R_\beta = \frac{\varphi_\beta y_w}{A_s W_{ax} \mu_{oil}} \end{cases} \quad (13)$$

In equation (13), y_w represents the water content of the emulsion; R_α means the rate at which the emulsion absorbs water; R_β is the rate at which the emulsion releases water; y_w^{max} represents the maximum water content of the emulsion; φ_α serves as the absorption coefficient of the oil spill; φ_β refers to the release coefficient of the oil spill; A_s and W_{ax} represent the content of asphalt and paraffin in the oil spill, respectively. The expression for the variation

of oil concentration in the water body of the spilled oil film is shown in equation (14).

$$N = \left(V\rho \sqrt{\frac{\pi}{4D_v t}} / A \right) \exp \left(-y \sqrt{\frac{\pi}{4D_v t}} \right) \quad (14)$$

In equation (15), N expresses the oil spill concentration (kg/m^3) at water depth y ; V means the volume (m^3) of the oil spill; ρ denotes the oil spill density (kg/m^3); t represents

time; D_v represents the vertical diffusion coefficient (m^2/s), and A refers to the area (m^2) of the oil film. The semi lethal concentration of the mixture can be obtained by combining the above formula with the pseudo component properties of dissolved aromatic hydrocarbons (Ruijter *et al.* 2020). The pseudo component properties of dissolved aromatic hydrocarbons are shown in Table 3.

Table 3. Pseudo component properties of dissolved aromatic hydrocarbons

pseudo-component	Molecular Weight(g/mol)	Solubility/ppm	Vapor pressure/atm	Log ₁₀
Monocyclic aromatic hydrocarbon	112	241.3	0.01526	3.2
Dicyclic aromatic hydrocarbons	141	16.9	6.20×10^{-4}	4.1
Tricyclic aromatic hydrocarbon	189	3.4	2.64×10^{-6}	4.7

Based on the proportion of different aromatic hydrocarbons in the oil spill, combined with different exposure times and temperatures, and combined with a superimposed toxicity model, the mortality rate of organisms can be calculated as shown in equation (15).

$$D = \frac{1}{\sqrt{2\pi}} \int_{-\infty}^Z \exp \left(-\frac{1}{2} \left(\frac{\log C - \log(LC50)}{\kappa} \right)^2 \right) du \quad (15)$$

In equation (15), D means the mortality rate of organisms; C denotes the environmental concentration (mg/L); Z represents the average deviation under normal seawater concentration, and κ represents the standard deviation for mortality. According to toxicity experiments, κ is generally set at 0.83. The damage caused by oil spills to the ecological environment can be evaluated using the ecological environment equivalence analysis method. The ecological environment equivalence analysis software developed by the National Coral Protection Association of the United States can calculate the area of damage and evaluate the monetary value of ecological environmental services based on the average cost of ecological restoration (Rehman Khan and Yu 2021). The most common ecological restoration project in China's coastal areas is mangrove restoration. Referring to the mangrove restoration cost of the Jimei Bridge, which is 25.68 yuan for an $1m^2$ sized mangrove, the

equivalent factor of mangrove serving the ecological environment in different ecological environments can be calculated (Hu *et al.* 2021). The equivalent factors relative to mangroves in different ecological environments are shown in Table 4.

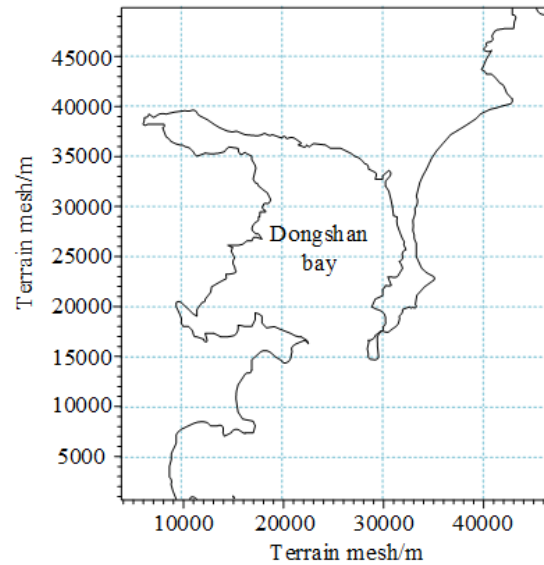


Figure 4. Grid simulation diagram

Table 4. Equivalent factors relative to mangroves in different ecological environments

Ecological environment type	Average public welfare value	Equivalence factor
Mangrove	9990	1
Coral reef	6075	0.608
Seagrass bed	22864	2.288
Rocky beach	1679	0.168

4. Example analysis of marine ecological loss assessment model for offshore oil extraction

To verify the effectiveness of the MEDA model for offshore oil extraction, the study used the oil spill accident in Dongshan Bay, Fujian Province as an example to set different operating conditions for verification. Surfer10.0 software was utilized to draw boundaries according to the longitude and latitude of $N23^{\circ}35'$, $N24^{\circ}03'$, $E117^{\circ}22'$, and $E117^{\circ}50'$ to generate coastal data files which were imported into MIKE21 software along with the hydrological

data of Dongshan Bay for grid division. It set the grid step size to 100m, the number of grid cells to 466×510 , the time step size to 30s, and the diffusion coefficient to a constant value of $20 m^2/s$. The resulting grid simulation diagram is shown in Figure 4.

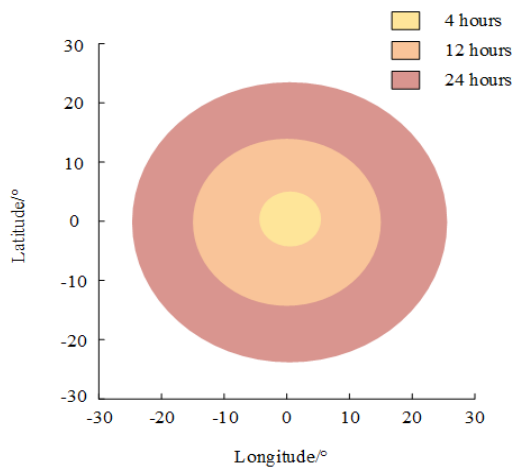


Figure 5. Simulation results of oil spill diffusion, drift behavior, and drift distance

In order to verify the effectiveness of the marine ecological damage assessment model for offshore oil extraction, simulation analysis was conducted on the diffusion of oil spills, drift behavior, and drift distance. The simulation results of oil spill diffusion, drift behavior, and drift distance are shown in Figure 5. From Figure 5, it can be seen that in the first few hours after the oil spill accident, the oil mainly spread near the accident area, and gradually drifted towards the surrounding waters due to the influence of ocean currents and wind speeds. Within 24 hours after the oil spill accident, the range of oil spill spread continuously expanded and the drift distance reached its maximum value. When the initial stage of oil spill is within 4 hours, the oil spill is mainly concentrated near the accident site and the diffusion range is relatively small. During the mid stage of oil spill, which lasts from 4 to 12 hours, the oil gradually spreads to the surrounding waters, and the drift distance increases significantly due to the influence of ocean currents and wind speeds. During the later stage of oil spill, which lasts from 12 to 24 hours, the diffusion range of the oil spill reaches its maximum value and the drift distance reaches its maximum. In summary, it can be seen that through the simulation analysis of the diffusion and drift behavior of oil spills, the model can accurately predict the diffusion and drift of oil spills in the sea area, further verifying the effectiveness and reliability of the evaluation model.

To verify the effectiveness of the MEDA model for offshore oil extraction, the model was used to simulate the flow

Table 5. Various parameters of oil spill

Project	Coefficient	Value	Project	Coefficient	Value
Emulsify	Maximum moisture content	0.85	Heat balance	Reflection coefficient	0.12
	Asphaltene content	0.05%		Oil radiation coefficient	0.80
	Wax content	5.70%		Atmospheric radiation coefficient	0.82
	Water absorption coefficient of emulsion	5×10^{-7}		Water radiation coefficient	0.95
	Emulsion water release coefficient	1.1×10^{-5}		Water temperature	20°C
Diffuse	Vertical diffusion coefficient	0.1465m ² /h		Atmospheric temperature	25°C
	Transverse diffusion coefficient	20m ² /s	Evaporation	Evaporation coefficient	0.028
	Longitudinal diffusion coefficient	20m ² /s	Dissolve	Solubility coefficient	2.35×10^{-6}

velocity and direction of the flow field with longitude and latitude (117°35.203'E,23°44.465'N), and compared with the actual flow direction and velocity of the flow field, as shown in Figure 6. From Figure 6 (a), the overall trend of the simulated flow velocity was basically consistent with the trend of the measured flow velocity. At a time of 64 minutes, the maximum error occurred between the simulated and the measured flow rates. At this time, the simulated flow rate was 0.71m/s, and the measured flow rate was 0.68m/s, resulting in a relative error of 4.31%. From Figure 6 (b), the trend of the simulated and measured flow directions was highly consistent. At the 43rd minutes, the maximum error occurred between the simulated and measured flow directions. At this time, the simulated flow direction was 0.81 °, while the measured flow direction was 0.84 °, resulting in a relative error of 3.63%. Overall, the error between the simulated flow direction and velocity of the MEDA model for offshore oil extraction and the actual situation did not exceed 5%, indicating the effectiveness of the model.

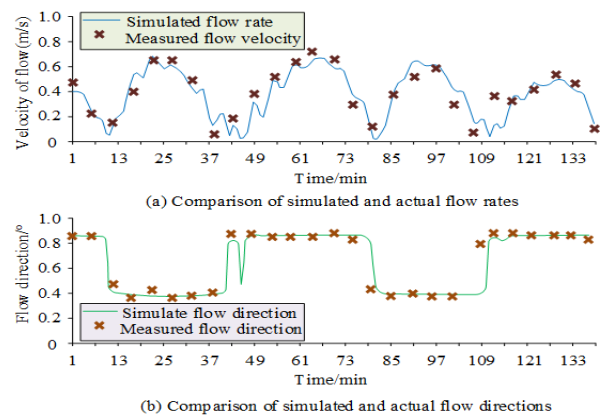


Figure 6. Comparison diagram of simulated and actual flow direction and velocity

To further validate the effectiveness of the MEDA model for offshore oil extraction, a flow field with latitude and longitude (117°34.29'E,23°47.29'N) was set as the simulated oil spill point, with an oil spill volume of 500t and an oil spill mode of instantaneous leakage. The oil spill during calm wind was set as condition 1, and the oil spill at a southeast wind speed of 3.1m/s was set as condition 2. The various parameters of the oil spill were simulated using the model, as shown in Table 5.

The MEDA model simulated the oil spill status after 72 hours under two operating conditions based on the above parameters, as shown in Figure 7. From Figure 7 (a), the oil spill in Condition 1 covered almost the entire Dongshan Bay area after 72 hours of calm wind, with only a small portion drifting out of the Dongshan Bay area. This indicated that during calm wind, the seawater rose in the Dongshan Bay area, hindering the outward diffusion of the oil spill. From Figure 7 (b), under the action of wind force, the oil spill in Condition 2 almost accumulated in the Dongshan Bay area after 72 hours. On the basis of Condition 1, Condition 2 only had an additional southeast wind force with a wind speed of 3.1m/s, indicating that this wind condition had a significant impact on the oil spill state.

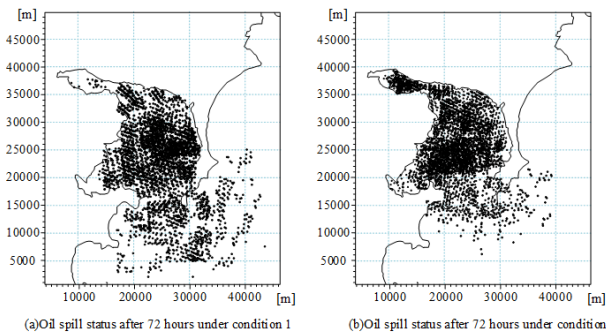


Figure 7. Oil spill status after 72 hours under two operating conditions

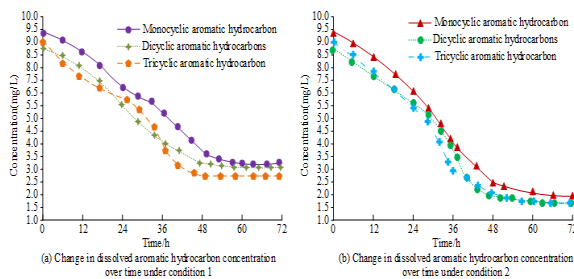


Figure 8. Changes in dissolved aromatic hydrocarbon

concentration within 72 hours under two operating conditions

To verify the ecological damage assessment performance of the MEDA model for offshore oil extraction, the areas with severe ecological damage in the Dongshan Bay area were selected, and the changes in dissolved aromatic hydrocarbon concentration within 72 hours under conditions 1 and 2 were verified, as shown in Figure 8. From Figure 8, the concentrations of monocyclic, bicyclic, and tricyclic aromatic hydrocarbons under different operating conditions gradually decrease with time, and the concentration curve gradually reached a stable state around 48 hours. From Figure 8 (a), the minimum concentrations of monocyclic aromatic hydrocarbons, bicyclic aromatic hydrocarbons, and tricyclic aromatic hydrocarbons reached in Condition 1 after 48 hours were 3.25mg/L, 3.02mg/L, and 2.78mg/L, respectively. From Figure 8 (b), the minimum concentrations of monocyclic aromatic hydrocarbons, bicyclic aromatic hydrocarbons, and tricyclic aromatic hydrocarbons reached in Condition 2 after 48 hours were 1.99mg/L, 1.74mg/L, and 1.73mg/L, respectively, which were reduced by 38.77%, 42.38%, and

37.77% compared to Condition 1. This indicated that the intensity of dissolved aromatic hydrocarbon damage in the water under Condition 2 was lower than that under Condition 1. This was because that wind speed accelerated the evaporation and volatilization of aromatic hydrocarbons in the oil spill, which reduced the concentration of dissolved aromatic hydrocarbons in the water body.

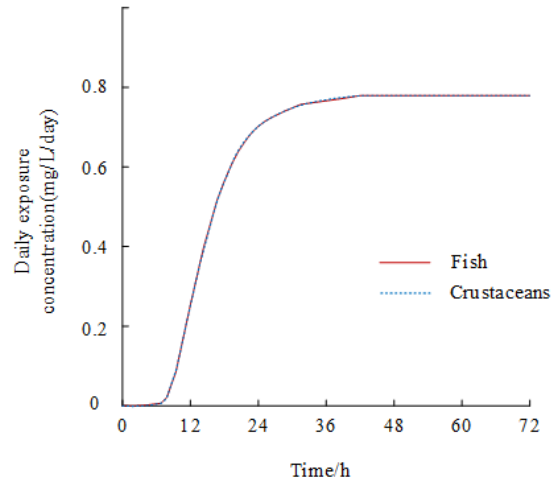


Figure 9. Exposure process of aquatic organisms

In order to more accurately evaluate biological losses, the study combines the migration and transformation of pollution with biological exposure processes to calculate the losses of fish and crustacean aquatic organisms. The study utilized the Monte Carlo simulation method in Crystal Ball software (Oracle inc, California USA) to calculate the daily exposure of organisms. The exposure process of aquatic organisms is shown in Figure 9. From Figure 9, it can be seen that the exposure concentration of organisms to aromatic hydrocarbons increases linearly within 48 hours and gradually stabilizes after 48 hours. In addition, it can be seen that the exposure curves of fish and crustaceans show a highly overlapping state, and at 48 hours, the exposure concentration reached its highest, at 0.895mg/L/day. Based on the pollution migration situation in the above figure, it can be seen that the exposure level of aquatic organisms to pollutants reached its highest after 48 hours.

In order to comprehensively consider the dynamic distribution characteristics of aquatic organisms in time and space. The study divides water space into three spatial dimensions based on the vertical depth of the water: surface depth, center depth, and bottom depth. Set the temperature of the water body to 20 °C, and set the exposure time to three groups: 24 hours, 48 hours, and 72 hours. The fishery resources in Dongshan Bay show that fish and crustaceans account for 96% of the total, so only fish and crustaceans are considered when using marine ecological damage assessment models for aquatic loss assessment. In order to evaluate the mortality rate of aquatic organisms, the above calculation formula and the aromatic hydrocarbon pseudo composition data in Table 3 were first used to calculate the half mortality rate of organisms under different exposure times and aromatic

hydrocarbon concentrations of pseudo components, as shown in Table 6.

Table 6. Half lethal rate of organisms under different conditions

Pseudo-component	Environment	Half lethal concentration	
		Fish	Crustacea
	Monocyclic aromatic hydrocarbon	2.113	2.594
	Dicyclic aromatic hydrocarbons	0.567	0.495
	Tricyclic aromatic hydrocarbon	0.167	0.0769
Exposure time	24h	3.924	4.619
	48h	2.647	3.034
	72h	2.237	2.649
Spatial distribution characteristics	Surface depth	3.064	4.519
	Center depth	2.490	2.876
	Bottom depth	2.061	1.917

The marine ecological damage assessment model evaluates the mortality rate of organisms under different working conditions based on the half mortality rate data in Table 6, and the dynamic distribution characteristics in time and space are shown in Figure 10. From Figure 10 (a), under condition 1, the mortality rates of fish and crustaceans were 34.8% and 21.4%, respectively, 24 hours after the oil spill occurred. The mortality rate of organisms increased linearly 48 hours after the oil spill occurred. At this time, the mortality rates of fish and crustaceans reached 74.2% and 65.5%, respectively. After 72 hours of the oil spill, the mortality rates of fish and crustaceans were 89.8% and 80.6%, respectively. From Figure 10 (b), under condition 2, the mortality rates of fish and crustaceans after 24 hours of oil spill were 28.3% and 20.01%, respectively. After 48 hours of oil spill, the mortality rates of fish and crustaceans reached 72.03% and 61.8%, respectively. After 72 hours of oil spill, the mortality rates of fish and crustaceans were 87.98% and 80.01%, respectively. Overall, it can be seen that considering the dynamic distribution characteristics of time and space, the mortality rate of aquatic organisms under condition 1 is higher than that under condition 2. After 24 hours, the mortality rate of fish and crustaceans ranges from 20% to 35%, but after 48 hours, the mortality rate is mainly concentrated in the range of 60% to 80%. Therefore, timely emergency response within 48 hours after an oil spill is particularly important.

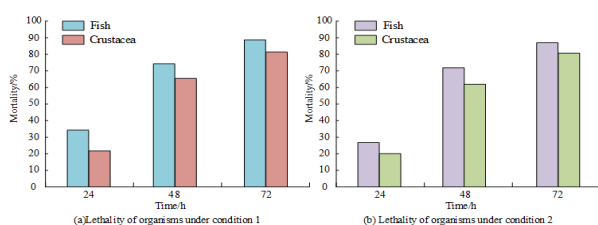


Figure 10. Lethality of organisms under different operating conditions

The calculated mortality rate can be multiplied by the local fishery resources to calculate the loss of local biological resources. The calculated resource loss of aquatic organisms under different operating conditions is shown in

Table 7. From Table 7, under condition 1, the total loss of the three types of aquatic organisms after 72 hours was 67.30 tons, and the losses after 24 and 48 hours were 20.29 tons and 45.13 tons, respectively, accounting for 30.15% and 67.06% of the total loss. Under condition 2, the total loss of three types of aquatic organisms after 72 hours was 56.03t, and the losses after 24 and 48 hours were 21.25t and 41.64t, respectively, accounting for 37.93% and 74.32% of the total loss. Overall, the loss of aquatic biological resources has reached over 30% of the total loss 24 hours after the oil spill occurred, so the time node for conducting ecological damage assessment of marine oil spills was particularly crucial.

Coral and mangrove protection areas are distributed in the Dongshan Bay area. The impact of oil spills on the ecological environment under different operating conditions is calculated using a MEDA model, as shown in Table 8. From Table 8, under condition 1, the ecological environment of coral and mangroves was affected by an area of 8.805km² and 5.859km², respectively, with a damaged service level of 26.655 and 8.091, and the ecological environment area that needs to be replaced was 0.831km² and 0.255km², respectively. Under condition 2, the ecological environment of coral and mangroves was affected by an area of 7.646 km² and 13.515 km², respectively, with a damaged service level of 23.05 and 18.67, and the ecological environment area that needs to be replaced was 0.725 km² and 0.584 km², respectively. From Table 4 above, the ecological environment of coral, with mangroves as the equivalent factor, was 0.608. Therefore, the alternative ecological environment area of coral in Condition 1 could be converted to 0.505km², and the total area of alternative ecological environment that needs to be constructed in Condition 1 was 0.760km². Similarly, the alternative ecological environment area of coral under Condition 2 was calculated to be 0.441 km², and the total area of alternative ecological environment that needs to be constructed under Condition 2 was 1.025 km². The cost of mangrove planting was calculated at 25.68/m² yuan, and the ecological environment resource losses caused by Condition 1 and Condition 2 were 19.5168 and 26.322 million yuan, respectively.

Table 7. Resource loss of aquatic organisms under different operating conditions

Exposure time	Working condition	Biomass loss/t			
		Fish	Shrimp	crabs	Amount to
24h	Condition 1	18.90	0.34	1.05	20.29
	Condition 2	19.81	0.38	1.06	21.25
48h	Condition 1	41.97	0.81	2.35	45.13
	Condition 2	38.79	0.80	2.05	41.64
72h	Condition 1	62.56	1.26	3.48	67.30
	Condition 2	52.16	1.12	2.75	56.03

Table 8. The impact of oil spills on the ecological environment under different operating conditions

Working condition	Condition 1	Condition 2
Affected coral ecological environment area/km ²	8.805	7.646
Affected mangrove ecological environment area/km ²	5.859	13.515
Total coral damage service level	26.655	23.059
Total mangrove damage service level	8.091	18.670
Area of coral alternative ecological environment/km ²	0.831	0.725
Area of mangrove alternative ecological environment/km ²	0.255	0.584

5. Conclusion

The oil spill accidents caused by offshore oil extraction activities have caused immeasurable damage to the marine ecological environment. To quantitatively evaluate the marine ecological damage caused by offshore oil extraction, a MEDA model was established based on the SIMAP model framework, and the MIKE21 model was added to the model construction to simulate the fate of the oil spill. At the same time, the ecological environment resource loss caused by oil spills was evaluated using the ecological environment equivalence analysis method. The results showed that the error between the simulated flow direction and flow velocity of the MEDA model for offshore oil extraction and the actual situation did not exceed 5%. After 48 hours, the minimum concentrations of monocyclic, bicyclic, and tricyclic aromatic hydrocarbons reached in Condition 2 were 1.99mg/L, 1.74mg/L, and 1.73mg/L, respectively, which decreased by 38.77%, 42.38%, and 37.77% compared to Condition 1. Under Condition 1, the mortality rates of fish and crustaceans were 34.8% and 21.4% after 24 hours of oil spill, 74.2% and 65.5% after 48 hours, and 89.8% and 80.6% after 72 hours, respectively. Under Condition 2, the mortality rates of fish and crustaceans after 24 hours of oil spill were 28.3% and 20.01%, respectively. The mortality rates after 48 hours were 72.03% and 61.8%, and the mortality rates after 72 hours were 87.98% and 80.01%, respectively. The total loss of the three types of aquatic organisms after 72 hours under condition 1 was 67.30 tons, while the total loss of the three types of aquatic organisms after 72 hours under Condition 2 was 56.03 tons. Under Condition 1, the ecological environment of coral and mangroves was affected by an area of 8.805km² and 5.859km², respectively, resulting in a loss of 19.5168 million yuan in ecological resources. Under Condition 2, the ecological environment of coral and mangroves was affected by an area of 7.646 km² and 13.515 km², respectively, resulting in a loss of 26.322 million yuan in ecological resources. In addition, the study analyzed the mortality rate of organisms under different working conditions by

combining temporal and spatial dynamic distribution characteristics, and showed that the mortality rates of fish and crustaceans were in the range of 20% to 35% after 24 hours, but the mortality rate was mainly concentrated in the range of 60% to 80% after 48 hours. Therefore, it can be concluded that timely emergency response within 48 hours after the occurrence of oil spills is particularly important. In summary, the MEDA model for offshore oil extraction studied has high assessment accuracy and has certain application value in the field of MEDA. The species of organisms in the ocean are complex and diverse, and research has not considered the toxicological characteristics of small base species with sensitive differences. Therefore, the experimental results are not comprehensive enough, and further improvement is needed in this regard.

Disclosures and declarations

Source of funds: None

Financial or non-financial conflicts of interest: None

References

- Abel S. and Spannowsky M. (2021). Quantum-field-theoretic simulation platform for observing the fate of the false vacuum, *PRX Quantum*, **2**(1), 10349, Aug.2021.
- Ardiada I.M.D., Feoh G., Adnyana G.F., Gunawan P.W., Bernadus I.N. and Rahayu P.W. (2022). Sistem Informasi Manajemen Akreditasi Prodi (Simap) Berbasis Web Dengan Instrumen Sembilan Kriteria Pada Universitas Dhyana Pura, *Jurnal Tika*, **7**(2), 165–176, Mar. 2022.
- Bigdeli M., Mohammadian A., Pilechi A. and Taheri M. and (2022). Lagrangian modeling of marine microplastics fate and transport: The state of the science, *Journal of Marine Science and Engineering*, **10**(4), 481, March, 2022. <https://doi.org/10.3390/jmse10040481>
- Chassé P. and Blatrix C. (2020). Frascaria-Lacoste What is wrong between ecological science and policy? *ECOL LETT*, **23**(12), 1736–1738, May. 2020. <https://doi.org/10.1111/ele.13613>
- Dukes E., Castner E., Leach A M., Galloway J.N., Lloret J., Messenger S. and Wietsma D. (2021). Introducing the nitrogen footprint in SIMAP: A review of improvements in

- nitrogen footprint methodology for institutions, *SCC*, **14**, (6), 415–423, <https://doi.org/10.1089/scc.2021.0048>.
- Hu P., Li F., Sun X., Liu Y., Chen X. and Hu D. (2021). Assessment of land-use/cover changes and its ecological effect in rapidly urbanized areas—Taking Pearl River Delta urban agglomeration as a case, *SUSTAINABILITY-BASEL*, **13**(9), 5075, Apr, 2021. <https://doi.org/10.3390/su13095075>
- Khan R., Ullah K. and Pamucar D. (2022). Performance Measure Using a Multi-Attribute Decision-Making Approach Based on Complex T-Spherical Fuzzy Power Aggregation Operators, *JCCE*, **1**(3), 138–146, Oct. 2022.
- Kralovec C. and Schagerl M. (2020). Review of structural health monitoring methods regarding a multi-sensor approach for damage assessment of metal and composite structures, *SENSORS*, **20**(3), 826, <https://doi.org/10.3390/s20030826>.
- Li L., He H., Jiang S., Qi J., Lu Y., Ding N. and Xiang X. (2021). Simulation of the in vivo fate of polymeric nanoparticles traced by environment-responsive near-infrared dye: A physiologically based pharmacokinetic modelling approach, *MOL*, **26**(5), 1271, February, 2021. <https://doi.org/10.3390/molecules26051271>
- Lima D.R., Carvalho C.R. and Garcia P.R.S. (2022). A criação do Sistema de Museus, Acervos e Patrimônio Cultural da UFRJ (Simap): desdobramentos de uma política cultural universitária, *R CPC*, **17**(33), 45–63, Jun. 2022.
- Maihulla A.S., Yusuf I. and Bala S.I. (2022). Reliability and performance analysis of a series-parallel system using Gumbel–Hougaard family copula, *JCCE*, **1**(2), 74–82, July. 2022.
- Nazuk A., Rashid M., Salman V. (2021). Optimizing Inventory Management Cost: Case of Simap, *Statistics, Computing and Interdisciplinary Research*, **3**(2), 99–116, March, 2021. <https://doi.org/10.52700/scir.v3i2.53>.
- Ng K.L., Opanchuk B., Thenabadu M., Reid M. and Drummond P. (2021). Fate of the false vacuum: Finite temperature, entropy, and topological phase in quantum simulations of the early universe, *PRX Quantum*, **2**(1), 10350, March, 2021. <https://doi.org/10.1103/PRXQuantum.2.010350>
- Rehman Khan S.A., Yu Z. (2021). Assessing the eco-environmental performance: an PLS-SEM approach with practice-based view, *International Journal of Logistics Research and Applications*, **24**(3), 303–321, Apr, 2021. <https://doi.org/10.1080/13675567.2020.1754773>
- Rosti M.E., Cavaiola M., Olivieri S., Seminara A. and Mazzino A. (2021). Turbulence role in the fate of virus-containing droplets in violent expiratory events, *Physical Review Research*, **3**(1), 13091, May. 2021.
- Rowen E.K., Pearsons K.A., Smith R.G., Wickings K. and Tooker J. (2022). Early-season plant cover supports more effective pest control than insecticide applications, *Ecological Application*, **32**(5), 2598, June, 2022. <https://doi.org/10.1002/eap.2598>.
- Ruijter V.N., Redondo-Hasselerharm P.E., Gouin and Koelmans A. Quality criteria for microplastic effect studies in the context of risk assessment: a critical review, *EST*, **54**(19), 11692–1705, Jun, 2020. <https://doi.org/10.1021/acs.est.0c03057>
- Veklych O., Karintseva O., Yevdokymov A. and Guillamon-Saorin E. (2020). Compensation mechanism for damage from ecosystem services deterioration: Constitutive characteristic *journal of Environmental Management*, **19**(1–3), 129–142, Apr. 2020.
- Verones F., Hellweg S., Antón A., Azevedo L., Chaudhary A., Cosme N. and Huijbregts M.A. (2020). LC-IMPACT: A regionalized life cycle damage assessment method, *Journal of Industrial Ecology*, **24**(6), 1201–1219, October, 2020. <https://doi.org/10.1111/jiec.13018>.
- Wenning R.J. and Tomasi T.D. (20230). Using US Natural Resource Damage Assessment to understand the environmental consequences of the war in Ukraine, *Integrated Environmental Assessment*, **19**(2), 366–375. <https://doi.org/10.1002/ieam.4716>.
- Yool A., Palmiéri J., Jones C G., Mor L. and Kuhlbrodt T.E. (2021). Popova & A. Sellar. Evaluating the physical and biogeochemical state of the global ocean component of UKESM1 in CMIP6 historical simulations, *Geoscientific Model Development*, **14**(6), 3437–3472, <https://doi.org/10.5194/gmd-14-3437-2021>
- Zan J. (2022). Research on robot path perception and optimization technology based on whale optimization algorithm, *JCCE*, **1**(4), 201–208, Nov.2022.